CrystEngComm

Accepted Manuscript

ROYAL SOCIETY OF CHEMISTRY

www.rsc.org/crystengcomm

Journal Name

RSCPublishing

ARTICLE

Room temperature agglomeration for the growth of BiTeI single crystal with giant Rashba effect

Cite this: DOI: 10.1039/xoxxoooooox

R. Sankar,[a] I. Panneer Muthuselvam,[a] Christopher John Butler,[b] S.-C. Liou,[a] B. H Chen,[a] M.-W. Chu,[a] W. L. Lee,[c] Minn-Tsong Lin,[d] R.Jayavel,[e] and F. C. Chou ,[*afg]

Received ooth January 2012,
Accepted ooth January 2012

DOI: 10.1039/xoxxoooooox

www.rsc.org/

We report a novel recipe of room temperature agglomeration (RTA) procedure to grow highly homogeneous and impurity-free BiTeI single crystals safely. The proposed four-step procedure of mixing and heating is able to prevent severe iodine loss and the danger of explosion for large scale crystal growth. Following the RTA treatment of the precursor, single crystals obtained from three different growth methods including vertical Bridgman, melt growth, and chemical vapour transport (CVT) were compared. Crystals grown with the Bridgman method showed the highest residual-resistance ratio (RRR) and mobility, and the largest domain size among the three. The crystal quality and purity has been confirmed using X-ray diffraction, Electron Probe Microanalysis (EPMA), Resistivity, TEM, and STM. Additionally, Mn intercalated and substituted BiTeI crystals have also been investigated.

Introduction

The Rashba effect, the spin-up and spin-down band splitting phenomenon in an external electric field, can be observed when the spin degeneracy originally protected by the time-reversal and inversion symmetries is lifted.[1] A surface energy gradient on structural inversion asymmetry in bulk materials can also provide a similar effect. Because it is desirable to fabricate devices that can be switched more quickly with spin, the Rashba effect in solids has a potential use in spintronics devices. However, the reported Rashba effect on material surfaces is usually too weak for practical application.[2] The recent finding of a giant Rashba effect in the layered material of BiTeI with strong inversion asymmetry has generated strong interest in the research community.[3-5] BiTeI has a layered structure in the space group of *P3m*1 (No. 156) (see Fig. 1), which lacks inversion symmetry as indicated by the ion ordering of Te- and I-layers on the opposite sides of Bi with unequal Bi-Te and Bi-I bond lengths. In particular, the spin band splitting of BiTeI described by Rashba energy ER (~100 meV) and Rashba parameter α_R (~3.8 eV Å) are at record high levels compared to those induced mostly by the surface energy gradient previously. Very recently, Rashba effect has also been observed in layered compound $LaOBiS_2$, which has similar spin splitting as BiTeI that originates from the polar field induced by the strong ionic bonding between atoms.[6] While Bi_2Te_3 has been demonstrated to show high thermoelectric figure-of-merit (ZT) for commercial applications,[7]

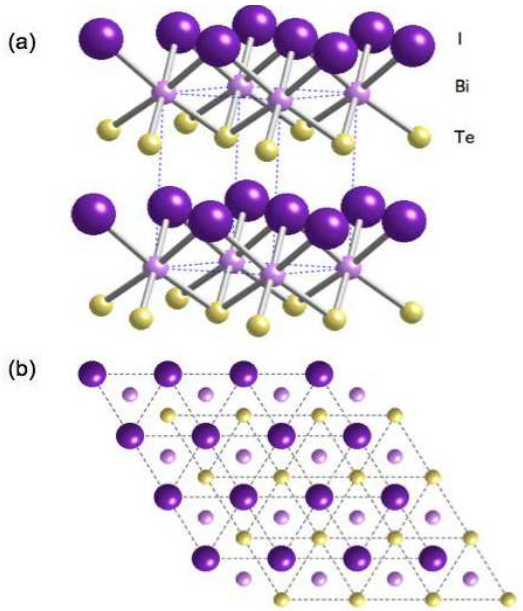

Fig.1 (a) BiTeI has a layered crystal structure of space group *P3m*1, which lacks inversion symmetry due to the ion ordering of Te and I on the opposite sides of Bi in hcp packing. (b) Te- and I-layers in c-projection for single tri-layer unit of BiTeI are shown to be a 2D triangular lattice.

BiTeI of similar layered structure has also been explored for its potential in thermopower improvement.[8] Temperature dependencies of the Seebeck coefficient have been explored in

BiTeBr and BiTeI,[9,10] but the thermal properties reported for the compound BiTeI are still limited. Bi_2Se_3 and Bi_2Te_3 have an identical crystal structure and are characterized as second-generation topological insulators, which have a surface band structure similar to that of graphene with a Dirac cone at the $\bar{\Gamma}$-point.[11] Both Bi_2Te_3 and Bi_2Se_3 show a quintuple layer building block with an identical Te/Se surface near the vander Waals gap.[12] On the other hand, BiTeI shows an interesting heterogeneous van der Waals gap that is formed by two different surfaces composed of Te and I atoms separately after the van der Waals gap is cleaved open.

The growth of impurity-free BiTeI crystal is challenging, mostly due to the easy sublimation nature of iodine solid at room temperature as a precursor, which becomes worse during the vacuum sealing of quartz tubing for on oxygen-free growth environment. The BiTeI samples used in the published works before often suffered from the impurity phase inclusion. For example, the single crystal BiTeI sample prepared by Ishizaka *et al*. contains a persistent BiI_3 impurity phase, unless a small amount of Mn was substituted in to the Bi site to eliminate the BiI_3 impurity phase and to improve crystal quality.[3] However, the impact of Mn substitution has not been explored fully, and the introduced Mn may have served as nucleation centers for the better growth. The difficulty of avoiding the BiI_3 impurity phase in BiTeI has even led to a complete thermoelectric property study on BiTeI samples with different amount of BiI_3 inclusion.[8] The published phase diagram of Bi_2Te_3-BiI_3 indicates that nonstoichiometry near the exact BiTeI ratio can be complicated by the existence of Bi/Te antisites and iodine defects.[13] Clearly, high purity BiTeI single crystal is highly desirable for both the fundamental and applied research fields. Herein, we report a unique growth recipe that grows impurity-free BiTeI single crystals through a newly designed room temperature agglomeration (RTA) procedure. The newly designed RTA procedure enhances the iodine handling safety significantly to avoid the danger of explosion of sealed quartz tubings during the heating process.

Recently Wang *et al.* reported the synthesis of BiTeI submicrometer hollow spheres by hydrothermal method,[14] and the report of BiTeI single crystal growth by Bridgeman method indicating several phase transitions under high pressure.[15] In large scale single crystal growth, the handling of iodine of low boiling point is very important during the heating and mixing process. We report a four-step procedure on mixing and heating to prevent the iodine loss and the danger of explosion, which is a novel recipe to grow highly homogenous and impurity-free single crystal BiTeI.

Material characterization

Powder X-ray diffraction was performed with crushed crystal samples in a Bruker-AXS D8 ADVANCE X-ray diffractometer which is equipped with a diffracted beam monochromator set for Cu $K_{\alpha 1}$ radiation (λ = 1.54056 Å) at room temperature. The structure refinement used data obtained from the synchrotron X-ray source in NSRRC-Taiwan. Chemical analysis was performed using electron microprobe analysis (EPMA). The transport properties for the BiTeI crystals were measured using a four-probe method for the in-plane resistivity as a function of temperature. Two types of specimens with the crystalline *c*-axis perpendicular and parallel to the sample plane were prepared for investigation. The sample with plane perpendicular to the *c*-axis was easily prepared by mechanical cleavage, whereas the sample with plane parallel to the *c*-axis was prepared by a standard cross-sectional technique followed by Ar^+ ion milling at 3 keV (Gatan PIPS). Both specimens were finally cleaned by low-energy ion milling at 0.3 keV to remove the possible surface amorphous layers. All electron diffraction patterns were acquired on a FEI field-emission electron microscope (TecnaiF20) operated at 200 kV. High-angle annular dark-field (HAADF) imaging in scanning transmission electron microscope (STEM) was performed on a JEOL-2100F microscope equipped with a probe spherical aberration corrector. Cleavage of all BiTeI crystal for investigations by scanning tunneling microscope (STM) was performed in a preparation chamber with a base pressure lower than 5 x 10^{-11} mbar. Crystals were cleaved on a L-He cooled cryostat, allowing a cleavage temperature of around 8 K. All STM measurements were performed at 4.5 K in an Omicron low temperature STM using a chemically etched tungsten tip. dI/dV intensity maps were acquired simultaneously with constant current topography images using a lock-in amplifier, with a bias modulation of 40 mV at frequency of 5.9 kHz.

Experimental details

In order to obtain the best recipe for the BiTeI growth, we have tried and compared three reaction routes of different precursor mixtures. While the iodine solid is easy to sublime during the vacuum sealing process, two types of precursors without direct iodine handling have also been tried, including the use of intermediate compounds BiI_3 and Bi_2Te_3. The three tested reaction routes are:

$$Bi_2Te_3 + BiI_3 \rightarrow 3BiTeI \quad (1)$$
$$BiI_3 + 2Bi + 3Te \rightarrow 3BiTeI \quad (2)$$
$$Bi + Te + I \rightarrow BiTeI \quad (3)$$

Reaction (1) requires the use of both pre-reacted Bi_2Te_3 and BiI_3. Reaction (2) uses pre-reacted BiI_3 plus Bi and Te metal. Reaction (3) uses the raw materials of I_2 crystal, Te and Bi solids directly, but it must be cautioned that a purification process is necessary before mixing, especially for the iodine.

Melt growth of BiTeI single crystal

We applied the same preliminary steps of room temperature agglomeration (RTA) procedure and high temperature homogenization for all three reaction routes as shown above. Single crystal growth of BiTeI containing the iodine element must be separated into several steps, instead of mixing and melting in one step to avoid potential explosion and impurity

formation. The regent grade ingot of Bi metal and Te metal crystal must be purified several times before weighing and mixing. Purification process has been applied to each element sealed in evacuated quartz tubing using a zone refining method for five times. Each element is melted at 650 ^{o}C in zone-I for 6 hrs first and recrystalized at zone-II which is kept at 550 ^{o}C by keeping the tube tilted at an angle of 40^{o}. Sublimation process used to purify iodine crystal. BiI_3 and Bi_2Te_3 precursors were prepared starting from the reaction of stoichiometric mixtures of Bi, I_2, and Te at 450°C (for BiI_3) and 600°C (for Bi_2Te_3) accordingly for 24 hours in an evacuated quartz ampoule. These mixtures were filled into a conical tip quartz ampoule in the glovebox and evacuated under pure argon atmosphere at 20 mTorr. Two different annealing temperatures of 550 and 600 °C were tested in order to compare the potential iodine nonstoichiometric. For the melt growth method growth, final cooling was done from 550/600 to 400 °C at a rate of 1.5 °C/hr followed by furnace cooling to room temperature. The obtained crystals were plate-like with the *c*-axis parallel to the vertical direction. The as-grown crystals were found easy to cleave along the (00l) plane of mirror-like quality, as shown in Fig. 3. The typical crystal size is ~3 cm in length and ~1 cm in diameter.

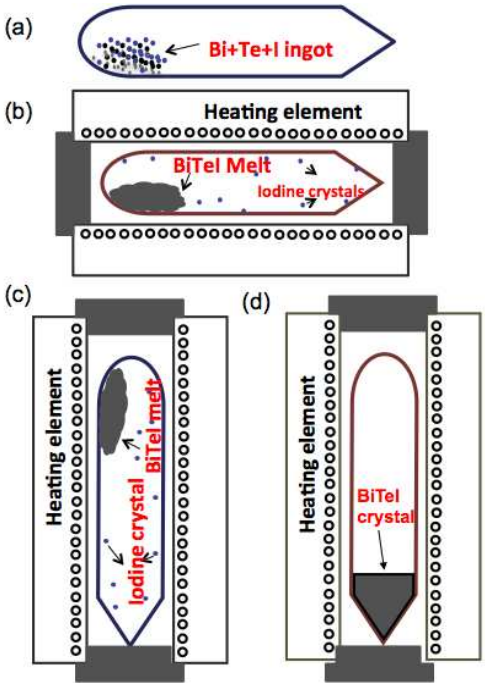

Fig.2 Melt growth procedures for single crystal BiTeI. (a) Step 1: room temperature agglomeration, (b) Step 2: horizontal high temperature annealing, (c) Step 3: vertical high temperature annealing, and (d) Step 4: slow cooling crystal growth.

We can summarize the melt growth conditions in four steps below (see Fig.2) :

Step 1. Room temperature agglomeration:

A total weight of ~5 grams of stoichiometric and purified precursors are mixed and sealed in a quartz ampoule of 1.8 cm inner diameter and ~20 cm in length in a glovebox. The sealed ampoule is placed in a horizontal furnace at room temperature for 24 hours to allow iodine to intercalate into Bi/Te and react homogeneously, which is the key procedure to avoid quartz tube explosion upon heating, especially for reaction (3).

Step 2. Horizontal high temperature annealing:

The ampoule is placed in a horizontal furnace at a small tilt angle, annealed at 550/600 °C for 24 hours with a heating rate of 50 °C/hr. The BiTeI melt can be observed at the bottom of the ampoule and small iodine crystals can be seen on the wall of the quartz ampoule after cooling.

Step 3. Vertical high temperature annealing:

The same ampoule is placed in a vertical tube furnace with the conical tip pointing downward, heated to 550/600 °C for 24 hours with a heating rate of 50 °C/hr. This step ensures that the precipitated iodine crystals on the wall fully react with the fux.

Step 4. Slow cooling crystal growth:

After the completion of Step 3 of high temperature annleaning, slow cooling between 600- 400˚C at a rate of 1.5˚C/hr ensures crystal growth occurs starting from the nucleation at the relatively colder point tip below. Finally, the ampoule is cooled down to room temperature a rate of 10˚C/hr after the crystal growth is completed below 400℃.

Bridgman growth of BiTeI single crystal

BiTeI single crystals were prepared from the bismuth, tellurium and iodine 5N purity elements. The synthesis of the compounds was carried out in conical quartz ampoules evacuated to 20 mTorr. The homogenization of the batches and synthesis of the compounds was carried out identically to the melt growth up to the Step 3 described above. Before the Bridgman method pulling, the ampoules containing the melt were heat-treated at 600°C for 24 h to ensure the melt filled the tip of ampoule first, the ampoules were then lowered through the temperature 600 °C of gradient 1 °C/cm at a rate of 0.1 mm/h. The obtained BiTeI single crystals were 3 cm long and 1.2 cm in diameter, which is easy to cleave to expose the (001) plane. This growth method gave homogeneous single crystals and the (001) plane is always perpendicular to the pulling direction.

Chemical vapour Transport growth of BiTeI single crystal

CVT growth of BiTeI crystals was carried out with a quartz ampoule of 45 cm length and 18 mm in diameter. The solidified melt precursor was prepared following the Step 3 treatment identical to the melt growth procedure described above. The quartz ampoules charged with melt precursor were rinsed with pure argon and evacuated to a pressure of 26.7 Pa. Single crystals were transported from the hot zone between 550 °C (T1) and 525 °C (T2) in 15 cm, to the cold zone at 500 °C (T3). The crystals were easy to cleave and with large shiny surfaces of (001) crystal plane.

Results and discussions

Single crystal samples grown with three different methods are shown in Fig. 3. The as-grown pure BiTeI crystal is stable in the air and can maintain its cleaved shiny surface for hours in the air without degradation. The room temperature powder X-ray diffraction patterns for melt growth crystals from three different reaction routes are compared in Fig. 4. It is clear that except for reaction (3) of direct Bi+Te+I initial mixing, the other routes contain Bi_2Te_3 and BiI_3 impurity phases. We find that Mn_xBiTeI crystals become hygroscopic after being stored in the air for one day, as evidenced from the build-up of a layer of brown colored film which is confirmed to be $MnI_2.4H_2O$. On the other hand, an $MnTe_2$ impurity phase is commonly observed in the growth of $Bi_{1-x}Mn_xTeI$ crystals, although it has been reported that minor Mn substitutions could improve the crystal quality of BiTeI.[3]

Fig.3 Single crystals grown from three different growth methods, (a) melt growth, (b) chemical vapor transport (CVT), and (c) Bridgman growth. Bridgman growth of Mn_xBiTeI (x=0.1) is shown in (d) after it is stored in the air for one day. A thin brown film is coated on the surface to indicate that the sample is hydroscopic for Mn_xBiTeI.

The lattice parameters from X-ray diffraction and EPMA chemical analysis for crystal grown with Bridgman, Melt growth, and CVT methods are summarized in Table 1 and 2, respectively. The lattice parameters indexed with space group *P3m*1 agree with those published in the literature, especially for the Bridgman growth.[3] There is no significant difference on the chemical composition for crystals grown by the three different growth methods, although the melt growth crystal shows slightly larger *c*-axis which indicates possible iodine intercalation. The homogeneity and stoichmetry has been confirmed from EPMA chemical analysis through five point average and normalization to Bi.

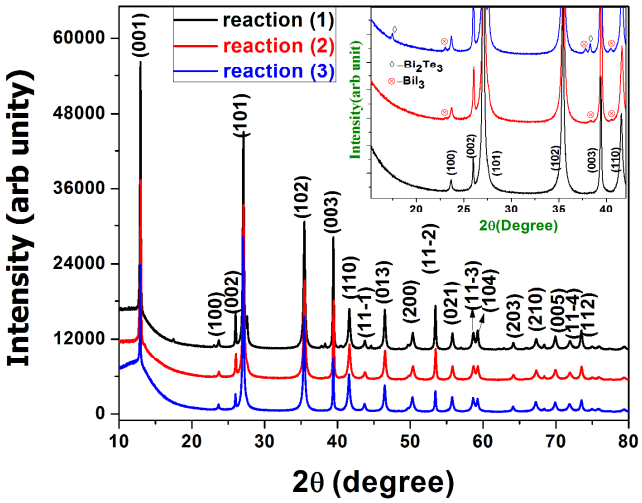

Fig.4 Powder X-ray diffraction patterns of melt growth BiTeI crystals grown using three different reaction routes are compared. As indicated in the inset, only the reaction (3) of direct Bi+Te+I mixing can avoid the formation of the BiI_3 impurity phase.

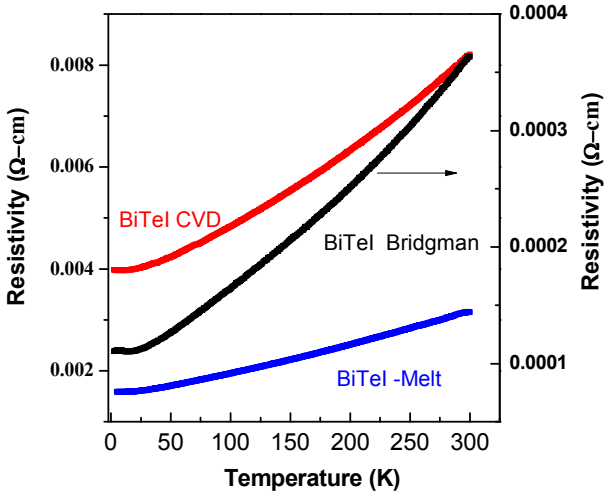

Fig.5 The in-plane resistivity as a function of temperature indicates that the Bridgman growth method provides crystals of the lowest resistivity and the highest RRR to indicate the best quality.

The in-plane resistivity data for single crystal BiTeI samples obtained from three growth methods are compared in Fig. 5.

Temperature dependence of resistivity ρ indicates that all samples show metallic behaviour. High residue resistivity below 10K is found for the crystals grown from the melt growth and CVT methods. On the other hand, the Bridgman growth crystal shows ρ at least one order lower and the RRR~4 is the highest among the three methods, which suggests that the Bridgman growth has the best quality with the least amount of impurities and crystallographic defects. Details of the Hall effect and Shubnikovde Haas quantum oscillation measurement results have been reported separately.[16]

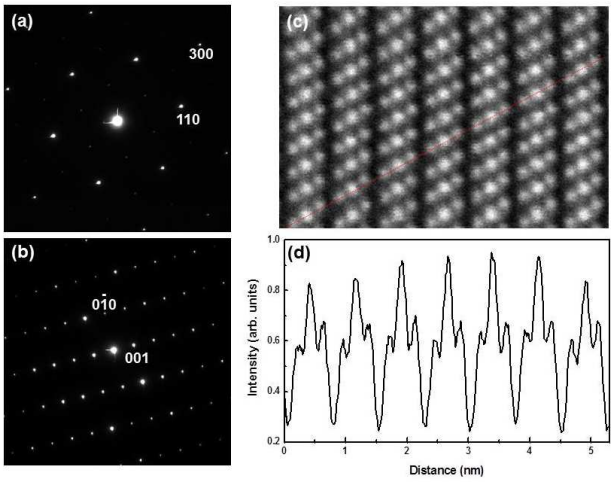

Fig.6 (a)-(b) The selected-area electron diffraction (SAED) patterns of single-crystal BiTeI acquired with the incident electron beam parallel to the c-axis along [001] direction and perpendicular to the c-axis along [-110] direction. (c) Shows the HAADF image along [-110] direction, and (d) shows the intensity profile measured along the red-dash line in (c).

Table 1: Lattice parameters of BiTeI single crystals from different growth methods

Growth method	a(Å)	b(Å)	c(Å)
Bridgman	4.3435	4.3435	6.8547
Melt growth	4.3421	4.3421	6.8835
CVT	4.3482	4.3482	6.8358

Table 2: The EPMA results obtained from the average of five selected points and normalize to Bi, as indicated in ratio of Bi:Te:I

Growth method	Bi	Te	I
Bridgman	1	1.0000(0.0010)	1.000(0.003)
Melt growth	1	0.9985(0.0019)	0.993(0.002)
CVT	1	0.9997(0.0014)	1.093(0.007)

The selected-area electron diffraction (SAED) patterns of single crystal BiTeI are shown in Fig. 6(a)-(b), which were acquired with the incident electron beam parallel to the *c*-axis along the [001] direction and perpendicular to the *c*-axis along the [-110] direction, respectively. Both SAED patterns indicate that the crystallinity is expected for the single phase single crystal. The STEM-HAADF imaging with atomic column resolution has been used to investigate the real-space structural arrangement of BiTeI. The representative HAADF image along [-110] direction of BiTeI is shown in Fig. 6(c), and the corresponding intensity profile measured along the red-color dash line in Fig. 6(c) is shown in Fig. 6(d). The triple-stacking-layer structure of BiTeI and the van der Waals gaps are displayed clearly in agreement with the assigned space group. Because the bismuth has a much larger atomic number than those of tellurium and iodine (Bi: Z=83, Te: Z=52 and I: Z=53), the central columns of triple stacking layers with brighter contrast corresponds to the Bi atomic columns, and the others two columns are Te and I, respectively.

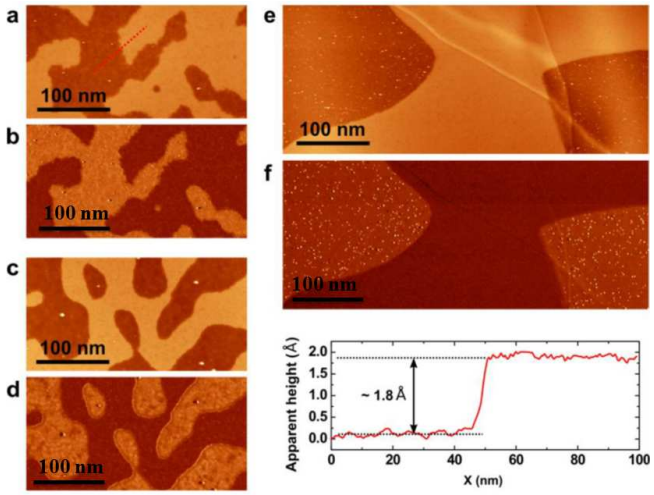

Fig.7 STM topography and dI/dV conductance maps of BiTeI taken on the vacuum cleaved surfaces of melt growth crystal ((a)-(b)), CVT crystal ((c)-(d)), and Bridgman crystal ((e)-(f)), respectively. All images are shown at the same scale. (g) Topographic line profile taken along the red dotted line in panel (a).

Scanning tunneling microscopy (STM) topography and dI/dV conductance images for crystals grown with three different methods are shown in Fig. 7. STM images acquired from vacuum-cleaved (001) surfaces of BiTeI crystals reveal a step-mesa morphology of two distinct domains separated by a step-height of around 1.8 Å. These steps are accompanied by a sharp contrast in conductance between domains, observed in simultaneously acquired dI/dV maps. This contrast is attributed to a difference in chemical termination between the two domains. As cleavage of the crystal is only expected to occur at the van der Waals gap between the Te and I atomic layers, the regions of different termination are thought to correspond to domains of inverse stacking sequence, resulting in a different atomic layer (Te or I) being uppermost at the surface after cleavage. The domains found at the surface of CVT and melt

grown crystals have typical scales of around 100 nm, and those found at surfaces of Bridgman grown crystals are much larger, with a scale of around 1 micro meter. The much larger domain size for the Bridgman growth crystal is consistent to its much lower resistivity (Fig.5) due to less scattering from the domain boundaries.

Conclusions

In summary, we have presented a safe and reliable growth recipe for the BiTeI single crystal to handle the iodine element which is easy to sublime during handling. The room temperature agglomeration procedure using a direct Bi+Te+I pristine elements is crucial to prevent potential explosions during the heating period for reaction in a sealed quartz ampoule. Single crystal BiTeI samples grown by three different methods have been fully characterized with X-ray diffraction, EPMA chemical analysis, electron diffraction, STM, and resistivity measurements, among which the Bridgman growth crystal has been shown to have the highest quality. We propose that the growth recipe with added room temperature agglomeration procedure can also be applied to the preparation of similar compounds that contain large amounts of iodine in the initial mixing process.

Acknowledgements

FCC acknowledges support from NSC-Taiwan under project number NSC 101-2119-M-002-007.

Notes

[a] Center for Condensed Matter Sciences, National Taiwan University, Taipei 10617, Taiwan.
[b] Department of Physics, National Taiwan University, Taipei 10617, Taiwan.
[c] Institute of Physics, Academia Sinica, Taipei 11529, Taiwan.
[d] Institute of Atomic and molecular Sciences,Academia Sinica,Taipei 10617,Taiwan.
[e] Anna University, Crystal Growth Centre, Chennai-600025,India,
[f] National Synchrotron Radiation Research Center, Hsinchu 30076, Taiwan,
[g] Taiwan Consortium of Emergent Crystalline Materials, National Science Council, Taipei 10622, Taiwan
E-mail: fcchou@ntu.edu.tw

References

(1) E. I. Rashba, *Sov. Phys. Solid State*,1960, **2**, 1109.
(2) P. King, R. Hatch, M. Bianchi, R. Ovsyannikov, C. Lupulescu, G. Landolt, B. Slomski, G. Balakrishnan, B. Iversen, J. Osterwalder, W. Eberhardt, F. Baumberger, and P. Hofmann, *Phys. Rev. Lett*, 2011 **107**, 096802.
(3) K. Ishizaka, M. S. Bahramy, H. Murakawa, M. Sakano, T. Shimojima, T. Sonobe, K. Koizumi, S. Shin, H. Miyahara, A. Kimura, K. Miyamoto, T. Okuda, H. Namatame, M. Taniguchi, R. Arita, N. Nagaosa, K. Kobayashi, Y. Murakami, R. Kumai, Y. Kaneko, Y. Onose, and Y. Tokura, *Nat Mater*, 2011, **10**, 521.
(4) V. Gnezdilov, P. Lemmens, D. Wulferding, A. Moller, 3 P. Recher, H. Berger, R. Sankar, and F. C. Chou, *Phy Rev B,* 2014, **89**, 195117.
(5) C. J. Butler, H. Yang, J. Y. Hong, S. H. Hsu, R. Sankar, C. Lu, H. Y. Lu, K. H. Ou Yang, H. W. Shiu, C. H. Chen, C. C. Kaun, G. J. Shu, F.C. Chou and M. T. Lin, *Nat. Commun,* 2014, **5**, 4066.
(6) Q. Liu, Y. Guo, and A. J. Freeman, *Nano Lett*. 2013, **13**, 5264.
(7) S. Scherrer and H. Scherrer, in Bismuth Telluride, Antimony Telluride, and Their Solid Solutions, edited by D. M. Rowe, CRC Handbook of thermoelectrics chap. 19 (CRC Press, 1995)
(8) V. A. Kulbachinskii, V. G. Kytin, A. A. Kudryashov, A. N. Kuznetsov, and A. V. Shevelkov, *J solid state chem*, 2012, **193**, 154.
(9) V. A. Kulbachinskii, V. G. Kytin, Z. V. Lavrukhina, A. N. Kuznetsov, A. V. Shevelkov, *Semiconductors,* 2010, **44**, 1548.
(10) V. A. Kulbachinskii, V. G. Kytin, A. A. Kudryashov, A. N. Kuznetsov, A. V. Shevelkov, *J. Solid State Chem*, 2012, **193**, 154.
(11) M. Z. Hasan and C. L. Kane, *Rev. Mod. Phys*, 2010, **82**, 3045.
(12) F.-T. Huang, M.-W. Chu, H. H. Kung, W. L. Lee, R. Sankar, S.-C. Liou, K. K. Wu, Y. K. Kuo, and F. C. Chou, *Phys. Rev. B*, 2012, **86**, 081104.
(13) A. Tomokiyo, T. Okada, S. Kawano, *Jpn. J. Appl. Phys*, 1977, **16**, 291.
(14) C. Wang, K. Tang, Q. Yang, J. Hu and Y. Qian, *J. Mater. Chem.* 2002, **12**, 2426.
(15) Y. Chen, X. Xi, W. Yim, F. Peng, Y. Wang, H. Wang, Y. Ma, G. Liu, C. Sun, C. Ma, Z. Chen, and H. Berger, *J. Phys. Chem. C,* 2013, **117**, 25677.
(16) C. Wang, J. Tung, R. Sankar, C. Hsieh, Y. Chien, G. Guo, F. C. Chou, and W. Lee, *Phys. Rev. B*, 2013, **88**, 081104.

